An Adaptive, Courant-number-dependent implicit scheme for vertical advection in oceanic models

Alexander F. Shchepetkin, UCLA

Honolulu, HI, February 25, 2014

Sec. 010 Physical and biogeochemical ocean modeling: development, assessment and applications. Kamehameha Hall III, poster # 16919

Abstract An oceanic model with an Eulerian vertical coordinate and an explicit vertical advection scheme is subject to the CFL limitation. Depending on the horizontal grid spacing, the horizontal-to-vertical grid resolution ratio, and the flow regime this limitation may easily become the most restrictive factor in choosing model time step. While terrain-following models are models of choice for the fine-resolution coastal modeling, often including tides interacting with topography resulting in large-amplitude baroclinic vertical motions, using terrain-following coordinate makes local vertical grid spacing depend on topography, ultimately resulting in very fine resolution in shallow areas in comparison with other models, z-coordinate, and isopycnic, which adds another factor in restricting time step. In this presentation we examine the possibility of mitigating vertical CFL restriction, while at the same time avoiding numerical inaccuracies associated with standard implicit advection schemes. In doing so we design a combined algorithm which acts like a high-order explicit scheme when Courant numbers are small enough to allow explicit method (which is usually the case throughout the entire modeling domain except just few "hot spots"), while at the same time has the ability to adjust itself toward implicit scheme should it became necessary to avoid stability limitations. This is done in a seamless manner by continuously adjusting weighting between explicit and implicit components.

Why to use implicit advection?
because it claims to overcome CFL limitation

Why not to use implicit advection?
because it is a gimmick and a lie

- it pretends to approximate terms in the equations *without actually advecting* what it is supposed to advect
- no Fourier component is allowed to change phase beyond π in one time step for *any* time stepping algorithm
- numerical dispersion is overwhelming in super-Courant regime forcing severe compromises and the necessity to dissipate
- even in sub-Courant regime the accuracy is no match to the best known explicit advection schemes
- spatial stencils are limited by complexity of implicit procedure; there are no known unconditionally stable time-stepping algorithms beyond second-order Crank-Nicolson (e.g. AM3 is asymptotically unstable)

Why to use implicit advection any way?
it is useful in situations when there is nothing left to advect

- it is *stratification* what fundamentally keeps vertical velocities small in the ocean; large vertical velocities occur when stratification is weak, negative, are correlated with strong mixing/convective adjustment events, interaction of tides with topography, tidally-enhanced mixing, etc.
- oceanic grids are very unisotropic, $\Delta z \ll \Delta x$, so large Courant number does not necessarily mean physically large vertical velocity
- unlike internal wave phase speeds and horizontal velocities, expected magnitude of vertical velocity is much harder to predict
- practical ROMS experience shows that starting with $\Delta x \leq 10km$ resolution vertical Courant number becomes the most restrictive factor. It is absolutely dominant in high-resolution 3D modeling involving tides
- vertical Courant numbers tend to be small everywhere, except very few places and during rare occasions: **very few "bad" grid points – "hot spots" – hold up simulations by imposing limit on Δt, while Courant number remains small elsewhere else**

Realistic example: Pacific 0.22^0 model

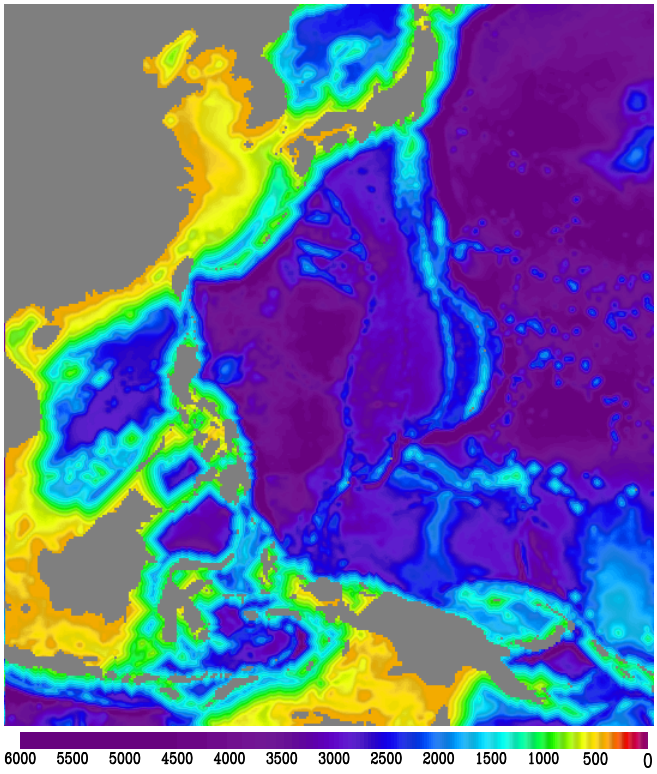

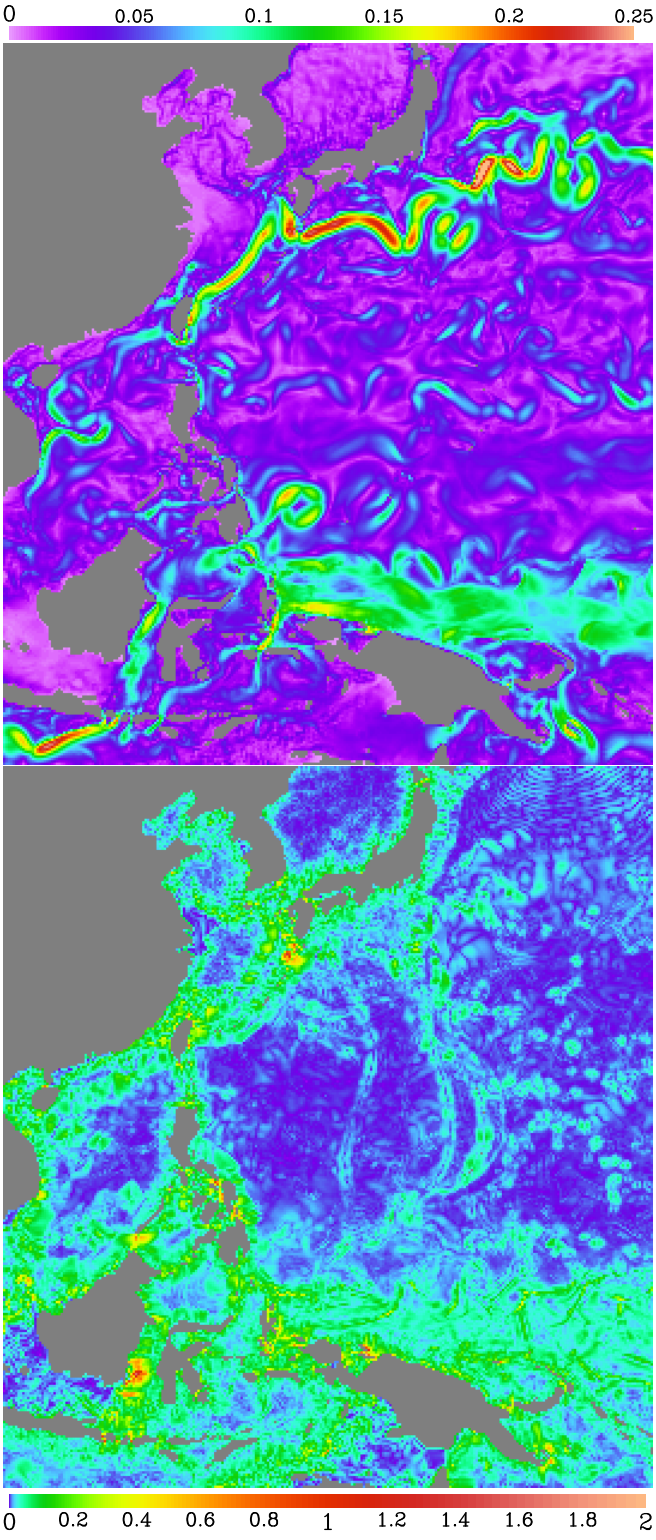

Model topography (*above*);
maximum values over each vertical column of:
top right – horizontal Courant number C_x;
right – vertical Courant number C_w (note stretched colorbar);
Grid resolution is $\Delta x = 25km \rightarrow 15km$, Equator $\rightarrow$ north, south;
$\Delta t = 2160s$

USWC L4 Palos Verdes configuration, $\Delta x = 75m$

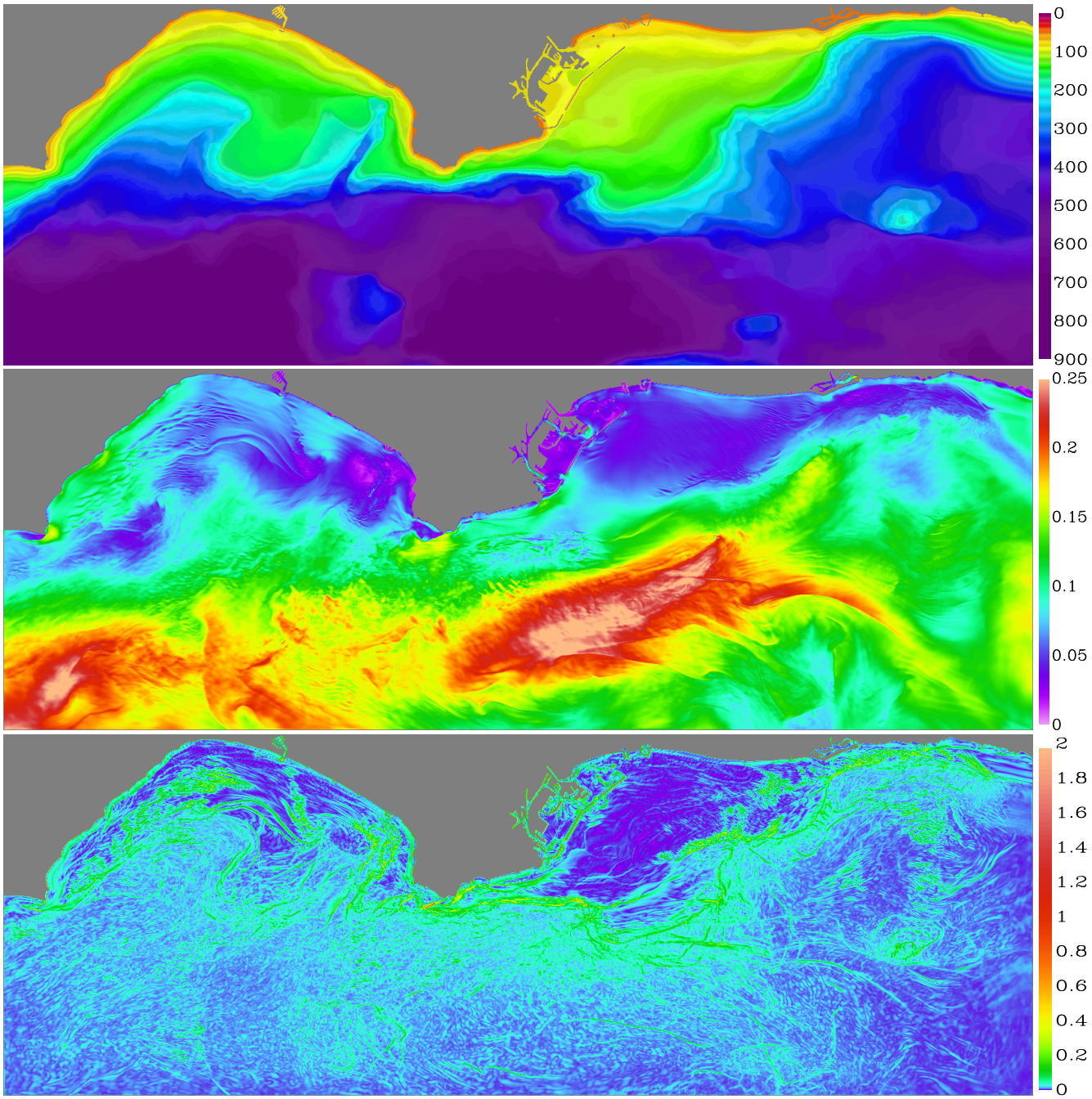

Top – Model topography; maximum values over each vertical column of: *middle* – horizontal Courant number C_x; *bottom* – vertical Courant number C_w. Grid resolution is $\Delta x = 75m$, $1600 \times 600 \times 32$ points. Maximum depth within this area is $900m$, minimum is only $2m$. This solution of forced by WRF modelled winds (atmospheric model $\Delta x = 6km$) and is tidally forced. Note stretched colobar of C_w – it is actually very small everywhere except near the tip of PV peninsula.

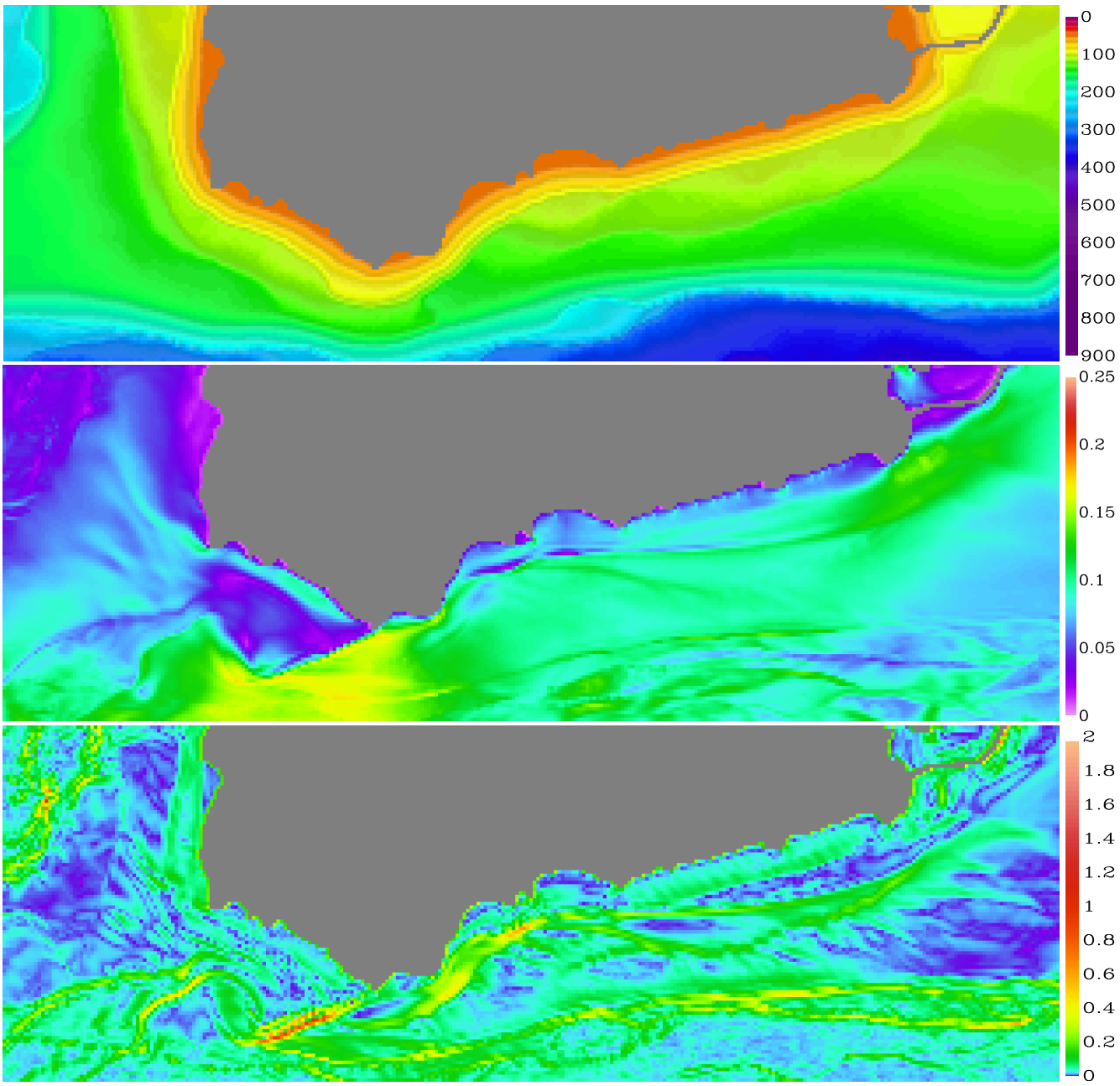

An enlarged portion of the previous figure.

The sole purpose of adaptive implicitness is to survive the situations like above.

Explicit and implicit advection at finite Courant numbers

Consider 1D advection

$$\partial_t q + c \cdot \partial_x q = 0$$

uniform $c = const$ discretized over uniform grid, $\Delta x = const$.

Flux-form update

$$q_j^{n+1} = q_j^n - \Delta t \left[F_{j+1/2} - F_{j-1/2} \right] \Big/ \Delta x \, .$$

$F_{j+1/2}$ needs interpolation of q to midpoints in space and proper time placement in order ensure temporal stability and accuracy of the algorithm – "effectively" at $n + 1/2$ to be least second-order.

Spatial: parabolic segment within each cell $x \in [x_j - \Delta x/2, x_j + \Delta x/2]$. An option for vertical advection in ROMS is to to compute vertical interface values by parabolic spline reconstruction. On a uniform grid

$$\frac{1}{6}\tilde{q}_{j-1/2} + \frac{2}{3}\tilde{q}_{j+1/2} + \frac{1}{6}\tilde{q}_{j-3/2} = \frac{q_j + q_{j+1}}{2}$$

to be solved for all half-integer-indexed $\tilde{q}_{j+1/2}$.

Time placement: use either time-space independent (method of lines, Hyman, 1979; ROMS LF-AM3 stepping belongs to this class), or time-space dependent (semi-Lagrangian in conservation form, van Leer, 1979, Colella & Woodward, 1984, Leonard, 1978,88,91).

LF-AM3 step: pre-step

$$q_j^{n+1/2} = \left(\frac{1}{2} - 2\gamma\right) q_j^{n-1} + \left(\frac{1}{2} + 2\gamma\right) q_j^n - \Delta t \cdot c\,(1 - 2\gamma)\, \frac{\tilde{q}_{j+1/2}^n - \tilde{q}_{j-1/2}^n}{\Delta x}$$

followed by $$q_j^{n+1} = q_j^n - \Delta t \cdot c \frac{\tilde{q}_{j+1/2}^{n+1/2} - \tilde{q}_{j-1/2}^{n+1/2}}{\Delta x}$$

$\gamma = 1/12$ for 3rd-order temporal accuracy.

Semi-Lagrangian using parabolic reconstruction,

$$F_{j+1/2} = c \left[\tilde{q}_{j+1/2}^n - \frac{\alpha}{2}\left(\tilde{q}_{j+1/2}^n - \tilde{q}_{j-1/2}^n\right) - \left(\tilde{q}_{j+1/2}^n + \tilde{q}_{j-1/2}^n - 2q_j^n\right)\left(\frac{3}{2}\alpha - \alpha^2\right) \right]$$

where $\alpha = c\Delta t/\Delta x$ is Courant number. It has many names, MUSCL, PPM, QUICKEST, etc...

Fourier component, $q_j^n = \lambda^n \cdot \widehat{q}_k \cdot e^{ik\Delta x j}$

Interpolation

$$\tilde{q}_{j+1/2} = \widehat{q}_k \cdot \frac{\cos(k\Delta x/2)}{(2/3)+(1/3)\cos(k\Delta x)} \cdot e^{ik\Delta x(j+1/2)}$$

Flux-differencing

$$\tilde{q}_{j+1/2} - \tilde{q}_{j-1/2} = \widehat{q}_k \cdot \frac{i\sin(k\Delta x)}{(2/3)+(1/3)\cos(k\Delta x)} \cdot e^{ik\Delta x j} = i\mathscr{K}\Delta x \cdot \widehat{q}_k \cdot e^{ik\Delta x j}$$

Taylor expansion

$$i\mathscr{K}\Delta x = ik\Delta x\left(1 - \frac{1}{180}(k\Delta x)^4 + ...\right)$$

fourth-order accurate. ...but this does not reveal the whole story.

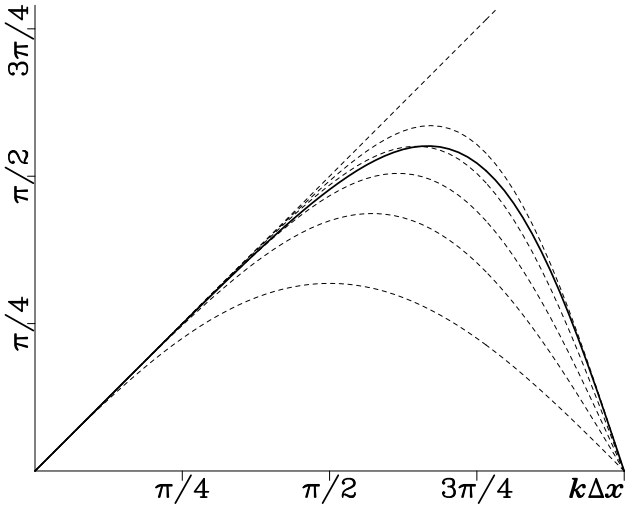

Fourier image $\mathscr{K} = \mathscr{K}(k\Delta x)$ of compact difference operator (**bold** curve) vs. that of conventional finite differences. Diagonal straight line is "ideal" $\mathscr{K}(k\Delta x) = k$; The five thin dashed lines are for the conventional non-staggered finite-difference schemes, starting with the second-order (*the lowest curve*), fourth-, sixth-, eighth-, and tenth-order (*the highest*). The maximum $\mathscr{K} = \sqrt{3}$ at $k\Delta x = 2\pi/3$

It has many fathers, most notably Kreiss (private communication acknowledged in Orszag and Israeli, 1974 and also in Hirsh, 1975), also known as Padé scheme and *compact* differencing.

Replacing flux-difference with $i\mathscr{K}(k\Delta x)$ in **LF-AM3 step** turns it into

$$\lambda^2 = 1 - \alpha^2(\mathscr{K}\Delta x)^2(1-2\gamma) - i\alpha\mathscr{K}\Delta x\left(\frac{1}{2}+2\gamma\right) - i\alpha\mathscr{K}\Delta x\left(\frac{1}{2}-2\gamma\right)\lambda^{-1}$$

which yields λ.

Dissipation per $1\Delta x$-travel $\quad |\lambda|^{(1/\alpha)}$

Numerical-to-ideal phase speed ratio

$$\lambda \equiv |\lambda| \cdot e^{\Delta\phi} \quad \text{ideally} \quad \lambda^{(\text{exact})} = e^{-i\alpha k\Delta x} \quad \text{hence} \quad \frac{c^*}{c^{(\text{exact})}} = \frac{\Delta\phi}{\alpha\, k\Delta x}$$

LF-AM3 step, $|\lambda|^{(1/\alpha)}$

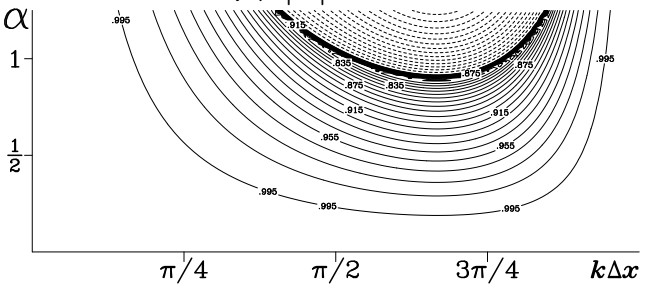

$c^*/c^{(\text{exact})}$

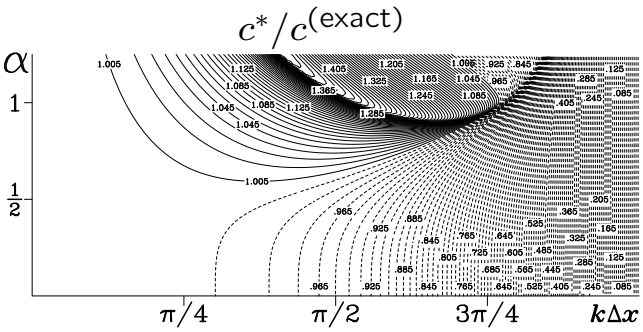

Ideally both $|\lambda|^{(1/\alpha)}$ and $c^*/c^{(\text{exact})}$ should be uniformly equal to 1. Contour interval is 0.01 in on both panels, however contour values are selected to be half-way between the integer multiples of the interval, so $|\lambda|^{(1/\alpha)} \equiv 1$ along both axes, $\alpha = 0$ and $k\Delta x = 0$, as well as along $k\Delta x = \pi$, while the entire area below, left and right from the lowest contour line (0.995 value) has values between 0.995 and 1 (hence within 0.5% less than the ideal). The white area on the lower-left portion of $c^*/c^{(\text{exact})}$ has values within the range of 1 ± 0.005.

Inserting $q_j^n = \lambda^n \cdot \widehat{q_k} \ldots$ and $\tilde{q}_{j+1/2} = \widehat{q_k} \cdot \ldots$ into **semi-Lagrangian** flux, and then the outcome into update for $q_j^{n+1} = \ldots$ yields

$$\lambda = 1 - i\alpha \cdot \frac{\sin(k\Delta x)}{(2/3) + (1/3)\cos(k\Delta x)} \cdot \left[1 - \frac{\alpha^2}{3}\Big(1 - \cos(k\Delta x)\Big)\right] \\ -\alpha^2 \cdot \frac{1 - \cos(k\Delta x)}{(2/3) + (1/3)\cos(k\Delta x)} \cdot \left[1 - \frac{\alpha}{3}\Big(1 - \cos(k\Delta x)\Big)\right]$$

where $i\mathscr{K}(k\Delta x)$ emerges again. Also $\alpha = 1$ turns it into $\lambda = \cos(k\Delta x) - i\sin(k\Delta x)$ which is exact – a typical semi-Lagrangian behavior.

Taylor expansion

$$\lambda = \underbrace{1 - i\alpha k\Delta x - \frac{\alpha^2(k\Delta x)^2}{2} + \frac{i\alpha^3(k\Delta x)^3}{6}}_{\text{match } \lambda^{(\text{exact})} = e^{-i\alpha k\Delta x}} + \underbrace{\left(\frac{i\alpha}{180} - \frac{\alpha^2}{24} - \frac{i-6}{72}\alpha^3\right)(k\Delta x)^4}_{\text{vs. } +\frac{\alpha^4(k\Delta x)^4}{24}} + \ldots$$

where $\frac{i\alpha}{180}$ acts against "true" $i\alpha$ causing phase delay (an inheritance of $i\mathscr{K}(k\Delta x)$), but is not typical dispersion because of $(k\Delta x)^4$ instead of $(k\Delta x)^3$; $-\frac{\alpha^2}{24}$ bends it inward at much higher rate than for would be purely rotational $-\frac{1}{2}\left(\frac{\alpha}{180}(k\Delta x)^4\right)^2$, hence dissipative (hyperdiffusive). However, it is quadratically vanishing – not what is expected from a semi-Lagrangian scheme: **this one does not dissipate when $\alpha \to 0$.**

semi-Lagrangian, $|\lambda|^{(1/\alpha)}$

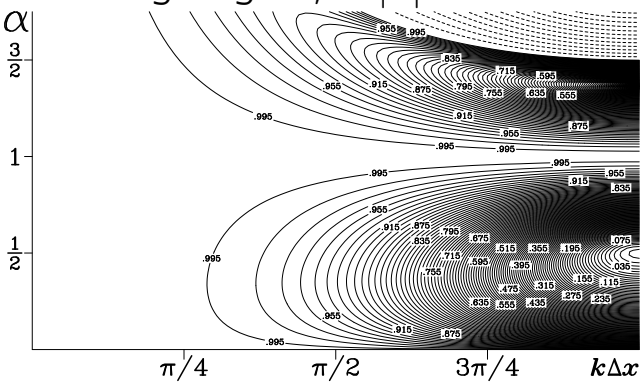

$c^*/c^{(\text{exact})}$

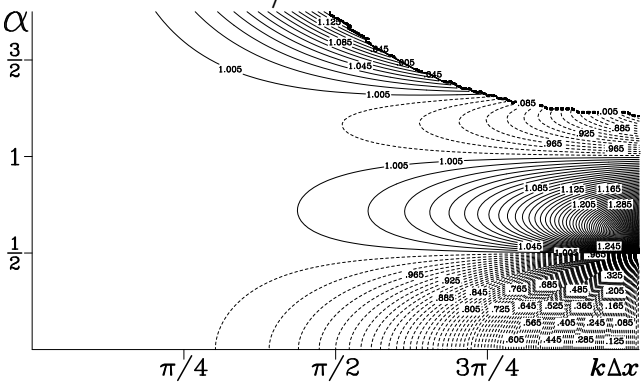

The area free of contour lines on the left portion of both $|\lambda|^{1/\alpha()}$ and $c^*/c^{(\text{exact})}$ plots is due to having values very close to 1: in the case of amplitude the left-most contour is 0.995, while the free area on the phase speed plot has values within the range of 1 ± 0.005. Because when $\alpha = 1$, $\lambda = \lambda(k\Delta x, \alpha)$ becomes exact, the free area is protruded all the way to the right in both plots along $\alpha = 1$ line (especially noticeable on $|\lambda|^{(1/\alpha)}$). The absence of contour lines in the upper-right corner of $c^*/c^{(\text{exact})}$ plot is die to the fact that $\text{Im}(\lambda)$ changes sign from negative to positive, which means that the phase angle cannot be uniquely defined on the portion of $(k\Delta x, \alpha)$ plane zero-contour line of $\text{Im}(\lambda)$, lower-left, due to π and $-\pi$ ambiguity. Dashed contours in $|\lambda|^{(1/\alpha)}$ correspond to $|\lambda| > 1$ – the algorithm is unstable within this area. Stability limit $\alpha_{\text{max}} = 3/2$. Dashed contours in phase speed plot indicate slower phase speeds relative to its exact value, while solid means moving faster. Note that when $\alpha = 1/2$ the phase error vanishes identically for all $k\Delta x$; also $|\lambda| = 0$ at $(k\Delta x = \pi, \alpha = 1/2)$ as it should, while the phase speed is discontinuous at this point resulting in contraction of contour lines.

Test Problem: advection of a narrow pulse

$$q(x)\Big|_{t=0} = \left[\cos\left(\frac{\pi}{2}\cdot\frac{x-x_0}{\sigma}\right)\right]^2 \quad \text{where} \quad \begin{cases} x \in [0,1]\,, & \Delta x = 1/256 \\ \sigma = 1/32\,, & x_0 = 3/4 \end{cases}$$

which is only $8\Delta x$-wide as measured at half of its height. Periodic boundaries on the left and right. The problem is run for one period: the pulse moves to the right, exits and re-emerges from the left, proceeds until reaching its initial position. The exact solution is the same as the initial state.

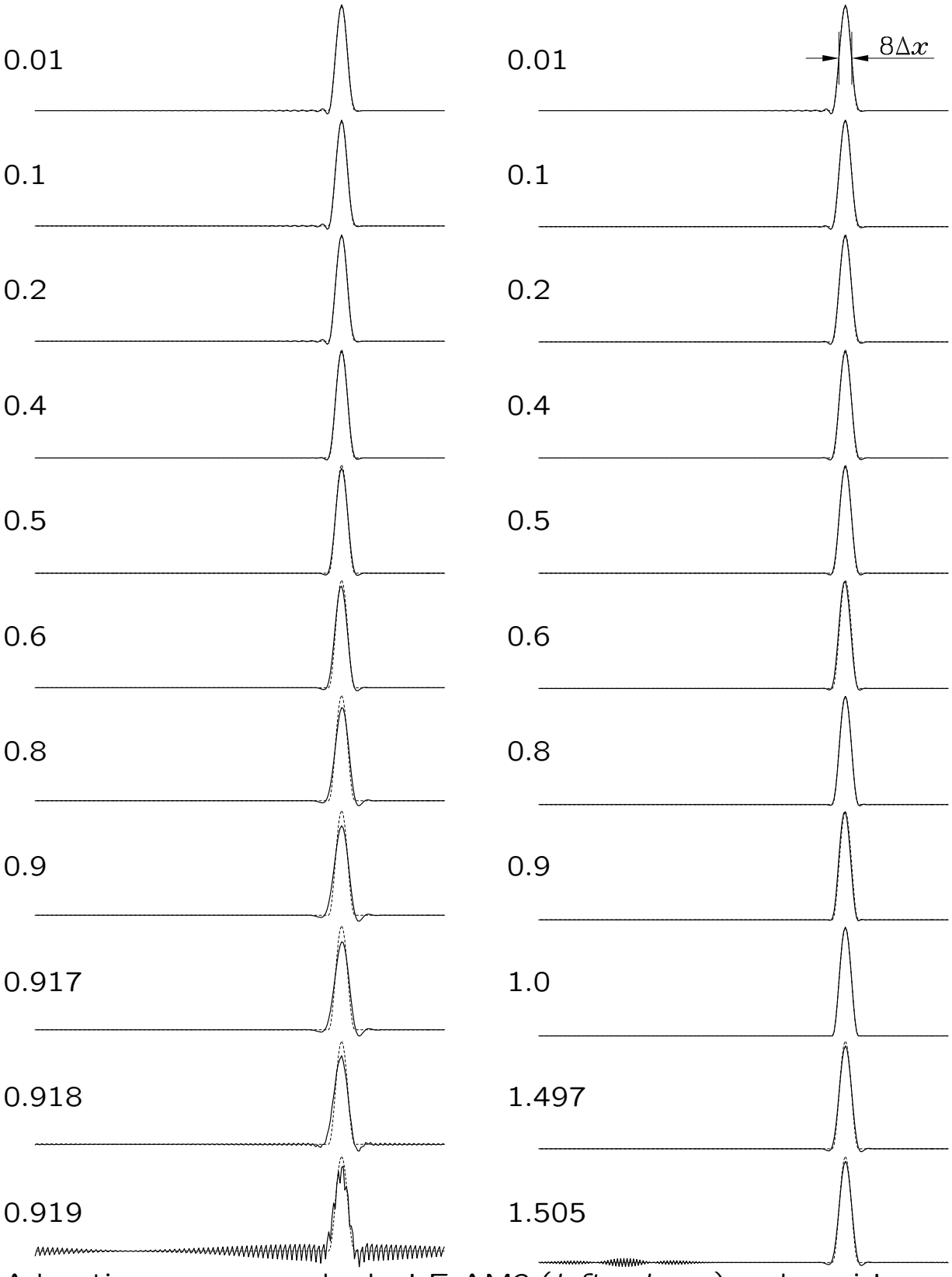

Advection a narrow pulse by LF-AM3 (*left column*) and semi-Lagrangian (*right*) algorithms. **Bold** line is numerical solution, *dashed* exact. Number on the left of each panel indicates Courant number, $c\Delta t/\Delta x$.

Implicit advection: Crank-Nicolson stepping

$$\frac{q_j^{n+1}-q_j^n}{\Delta t}+c\cdot\left\{\theta\cdot\frac{q_{j+1}^{n+1}-q_{j-1}^{n+1}}{2\Delta x}+(1-\theta)\cdot\frac{q_{j+1}^{n}-q_{j-1}^{n}}{2\Delta x}\right\}$$

step multiplier

$$\lambda=\frac{1-\alpha(1-\theta)\cdot i\sin(k\Delta x)}{1+\alpha\theta\cdot i\sin(k\Delta x)}$$

non-dissipative $|\lambda|\equiv 1$ if $\theta = 1/2$

Taylor expansion analysis

$$\lambda/\lambda^{(\text{exact})}=\lambda/e^{-ick\Delta t}\equiv\lambda/e^{-i\alpha k\Delta x}=+i\alpha\frac{(k\Delta x)^3}{6}+i\alpha^3\frac{(k\Delta x)^3}{12}+\ldots$$

only second-order in space, dispersive truncation error.

To repair this make a *compact* version of CN by "spreading" the time difference along x-direction,

$$\frac{q_{j-1}^{n+1}-q_{j-1}^n}{6\Delta t}+\frac{2}{3}\cdot\frac{q_j^{n+1}-q_j^n}{\Delta t}+\frac{q_{j+1}^{n+1}-q_{j+1}^n}{6\Delta t}$$
$$+c\cdot\left\{\theta\frac{q_{j+1}^{n+1}-q_{j-1}^{n+1}}{2\Delta x}+(1-\theta)\frac{q_{j+1}^{n}-q_{j-1}^{n}}{2\Delta x}\right\}$$

its step multiplier

$$\lambda=\frac{1-\alpha(1-\theta)\cdot\mathscr{K}(k\Delta x)}{1+\alpha\theta\cdot\mathscr{K}(k\Delta x)}$$

replaces $i\sin(k\Delta x)$ with $\mathscr{K}(k\Delta x)$.

C-N, 2nd-centered, $c^*/c^{(\text{exact})}$

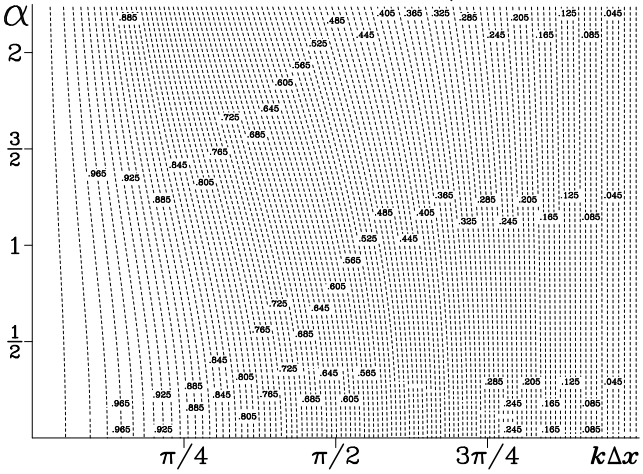

C-N, compact, $c^*/c^{(\text{exact})}$

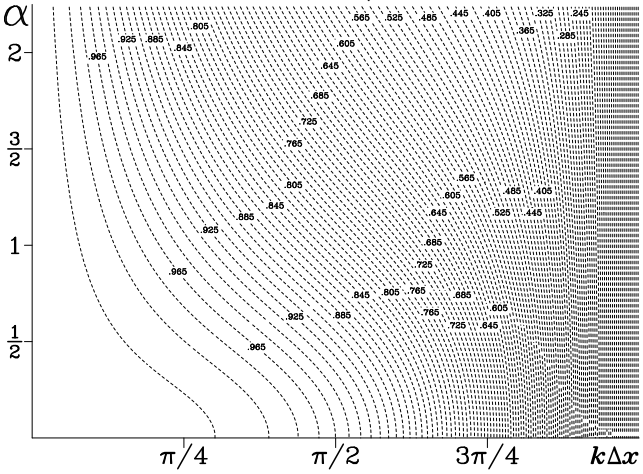

Overall major improvement for $\alpha \ll 1$; little gain for α beyond 1/2

Alternative: staggered in space, centered around $\left(x_j - \frac{\Delta x}{2}, t_n + \frac{\Delta t}{2}\right)$

$$\frac{q_j^{n+1} - q_j^n + q_{j-1}^{n+1} - q_{j-1}^n}{2\Delta t} + c \cdot \left\{ \theta \cdot \frac{q_j^{n+1} - q_{j-1}^{n+1}}{\Delta x} + (1-\theta) \cdot \frac{q_j^n - q_{j-1}^n}{\Delta x} \right\}$$

its step multiplier $$\lambda = \frac{\frac{1}{2} - (1-\theta) + \alpha\left(\frac{1}{2} + (1-\theta)\right) e^{-ik\Delta x}}{\frac{1}{2} + \theta \ \ + \alpha\left(\frac{1}{2} - \theta\right) e^{-ik\Delta x}}$$

unconditionally stable for $\theta \geq 1/2$

nondissipative, second-order in space-and-time for $\theta = 1/2$

coincidentally *exact* when $\alpha = 1$ (must be $\theta = 1/2$ as well)

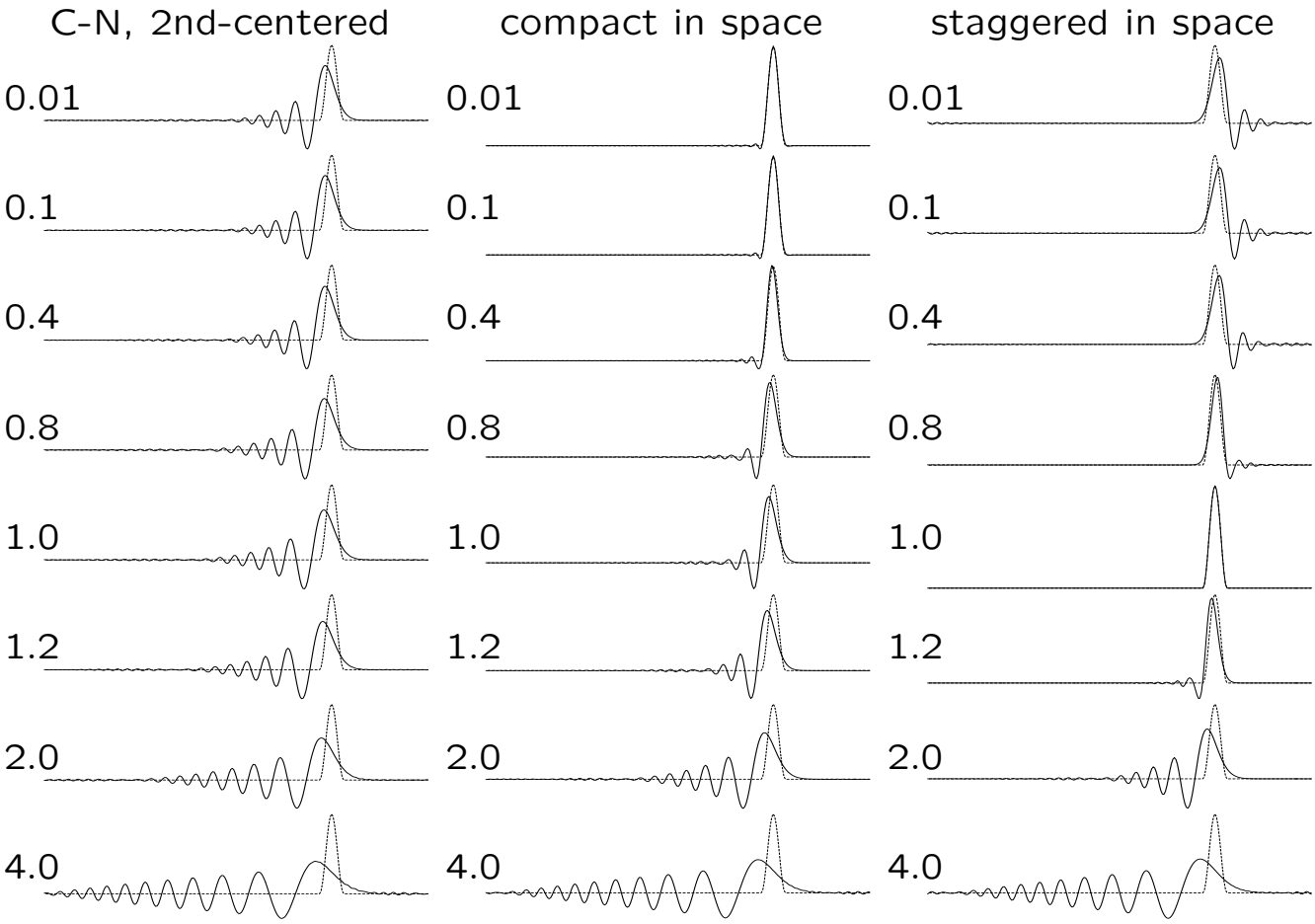

Advection and dispersive spreading of a narrow pulse by non-dissipative, unconditionally stable implicit schemes using different Courant number regimes. Equal-weight $\theta = 1/2$ Crank-Nicolson stepping in all three cases. *Left column* centered second-order differencing in space; *middle* compact-centered (fourth-order); *right* staggered in space, centered around $(x_j - \Delta x/2, y_n + \Delta t/2)$.

For small Courant numbers the middle-column is the most accurate; $\alpha = 1$ solution is exact in the right column, this scheme also produces the least dispersive spreading for $\alpha = 2$, however, all three schemes produce virtually the same dispersion for $\alpha = 4$ and above. Quadratic variance is maintained to machine accuracy by all three schemes in all cases.

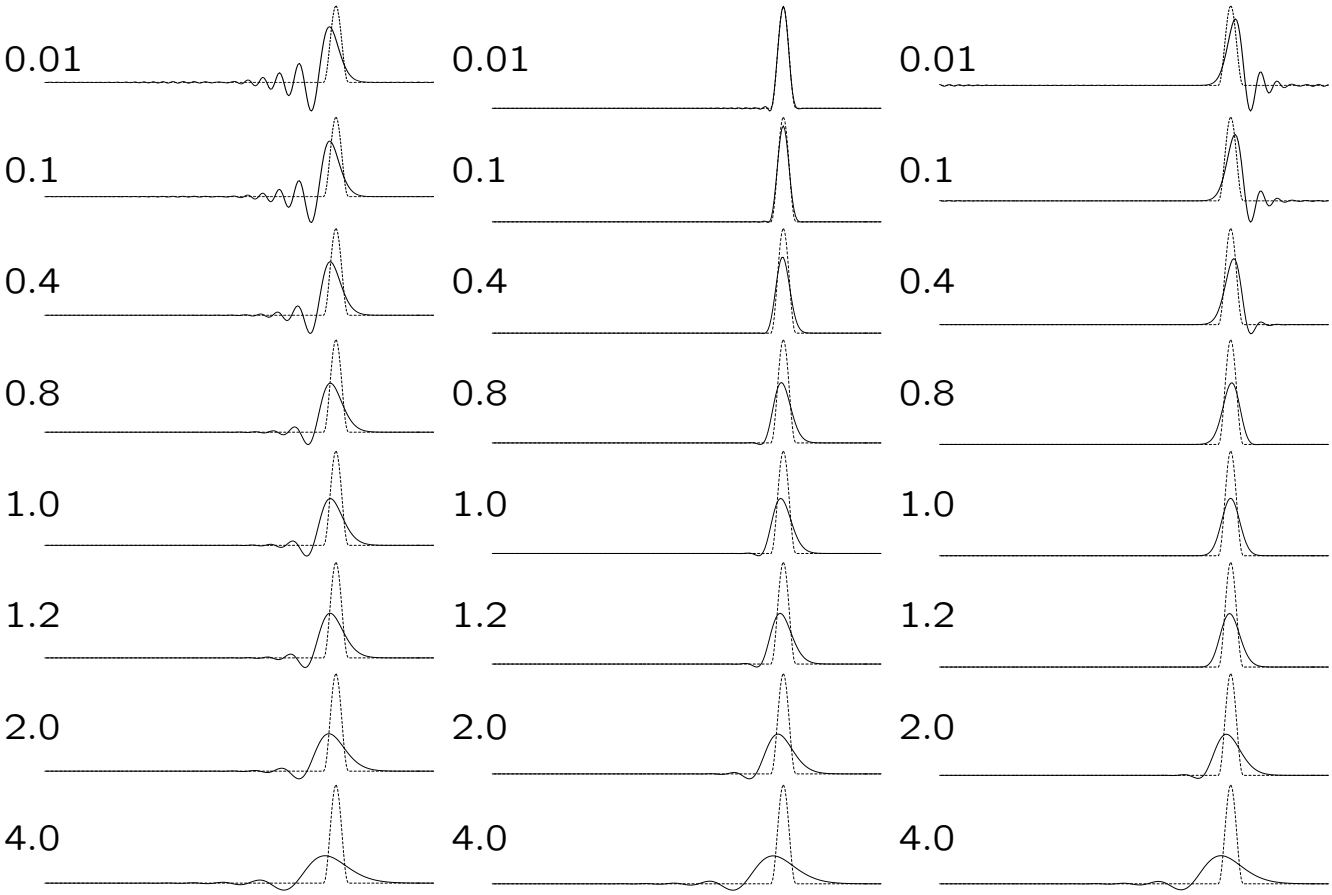

The same as previous, but for $\theta = 0.55$ in all three cases.

$\theta > 1/2$ makes little influence for small Courant numbers.

$\theta = 0.55$ vs. $\theta = 1/2$ makes virtually no change in dispersive properties, $c^*/c^{(\text{exact})}$, for the entire $k\Delta x, \alpha$-plane for all three schemes.

While for vanishingly small Courant numbers accuracy of an implicit scheme can be made comparable to explicit presented here, it deteriorates too quickly as α departs from there: eg at $\alpha = 0.4$ C-N with compact differencing is notably more dispersive if $\theta = 1/2$, or more diffusive, if $\theta = 0.55$ than either LF-AM3 or semi-Lagrangian. In contrast explicit schemes can be designed to be time-space accurate for the entire range of their stability. Dissipation in super-Courant regime is needed to control oscillations, however **θ-method is too non-selective**: way too much for $\alpha \sim 0.5$ and not enough beyond 1.

Overall direct application of any of these implicit methods does not seem to be attractive. We therefore need another approach.

Adaptively implicit vertical advection operator:

Vertical fluxes for the tracer or velocity fields are discretized involving the advected field at $n+1$ time step which are yet unknown,

$$FC_{k+1/2} = W_{k+1/2} \cdot \mathscr{Q}\left(q_k^{n+1}, q_{k\pm1}^{n+1}, q_k^{n+1/2}, q_{k\pm1}^{n+1/2}, ...\right)$$

rearrange by splitting vertical velocity into two parts,

$$W_{k+1/2} = W^{(e)}_{k+1/2} + W^{(i)}_{k+1/2}, \qquad \forall k = 0, 1, ..., N$$

where $W^{(i)}_{k+1/2}$ is for terms involving $q_k^{n+1}, q_{k\pm1}^{n+1}$ only (*i.e.*, implicit part), while $W^{(e)}_{k+1/2}$ for the remaining $q_k^{n+1/2}, q_{k\pm1}^{n+1/2}, ...$, then:

- **$W^{(e)}$-terms are computed within r.h.s via standard algorithm**

- **$W^{(i)}$-terms are integrated into the vertically implicit operator**

Assuming upstream treatment of the implicit part,

$$FC^{(i)}_{k+1/2} = W^{(i)}_{k+1/2} \cdot \begin{cases} q_k^{n+1}, & \text{if} \quad W^{(i)}_{k+1/2} > 0 \\ q_{k+1}^{n+1}, & \text{if} \quad W^{(i)}_{k+1/2} < 0 \end{cases}$$

the combined implicit advection-diffusion system becomes
$k = N$, uppermost grid box,

$$H_N^{n+1} q_N^{n+1} = H_N^n q_N^n + \Delta t \cdot \mathrm{rhs}'_N + \Delta t \cdot SRFRC - \Delta t A_{N-1/2} \frac{q_N^{n+1} - q_{N-1}^{n+1}}{\Delta z_{N-1/2}}$$
$$+\Delta t \left[\max\left(W^{(i)}_{N-1/2}, 0\right) q_{N-1}^{n+1} + \min\left(W^{(i)}_{N-1/2}, 0\right) q_N^{n+1}\right]$$

$k = 2, ..., N-1$

$$H_k^{n+1} q_k^{n+1} = H_k^n q_k^n + \Delta t \cdot \mathrm{rhs}'_k + \Delta t A_{k+1/2} \frac{q_{k+1}^{n+1} - q_k^{n+1}}{\Delta z_{k+1/2}}$$
$$-\Delta t \left[\max\left(W^{(i)}_{k+1/2}, 0\right) q_k^{n+1} + \min\left(W^{(i)}_{k+1/2}, 0\right) q_{k+1}^{n+1}\right]$$
$$-\Delta t A_{k-1/2} \frac{q_k^{n+1} - q_{k-1}^{n+1}}{\Delta z_{k-1/2}}$$
$$+\Delta t \left[\max\left(W^{(i)}_{k-1/2}, 0\right) q_{k-1}^{n+1} + \min\left(W^{(i)}_{k-1/2}, 0\right) q_k^{n+1}\right]$$

$k = 1$, bottom grid box,

$$H_1^{n+1} q_1^{n+1} = H_1^n q_1^n + \Delta t \cdot \mathrm{rhs}'_1 + \Delta t A_{3/2} \frac{q_2^{n+1} - q_1^{n+1}}{\Delta z_{3/2}}$$
$$-\Delta t \left[\max\left(W^{(i)}_{3/2}, 0\right) q_1^{n+1} + \min\left(W^{(i)}_{3/2}, 0\right) q_2^{n+1}\right]$$

The W-splitting works as follows: Compute $W_{k+1/2}$ the standard way; also compute finite-volume Courant number $\alpha_{i,j,k}$ at every grid box H_k as the sum of outgoing fluxes normalized by Δt and grid-box volume,

$$\alpha_{i,j,k} = \frac{\Delta t}{\Delta V_{i,j,k}} \cdot \Big[\max(FlxU_{i+1/2,j,k}, 0) - \min(FlxU_{i-1/2,j,k}, 0) + \max(FlxV_{i,j+1/2,k}, 0) - \min(FlxV_{i,j-1/2,k}, 0) + \max(W_{i,j,k+1/2}, 0) - \min(W_{i,j,k-1/2}, 0) \Big]$$

then the explicit part

$$W^{(e)}_{k+1/2} = \frac{W_{k+1/2}}{f(\alpha^*)}, \quad \text{where} \quad \begin{cases} \alpha^* = \alpha_k & \text{if} \quad W_{k+1/2} > 0 \\ \alpha^* = \alpha_{k+1} & \text{if} \quad W_{k+1/2} < 0 \end{cases}$$

and the limiting function

$$f(\alpha) = \begin{cases} 1\,, & \text{if} \quad \alpha \le \alpha_{\min} \\ 1 + \dfrac{(\alpha - \alpha_{\min})^2}{4\alpha_{\max}\,(\alpha_{\max} - \alpha_{\min})}\,, & \text{if} \quad \alpha_{\min} < \alpha < 2\alpha_{\max} - \alpha_{\min} \\ \alpha/\alpha_{\max}\,, & \text{if} \quad \alpha \ge \alpha_{\max} \end{cases}$$

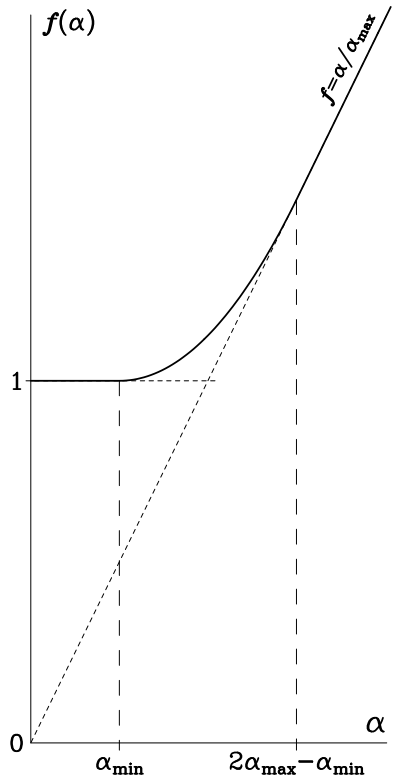

made of three segments – constant, parabolic, and linear – smoothly matched to each other; $\alpha_{\min}$ control the threshold below which the algorithm is fully explicit; $\alpha_{\max}$, and the maximum allowed Courant number **"never exceed speed"** for the explicit part The implicit part is the "excess" velocity

$$W^{(i)}_{k+1/2} = W_{k+1/2} - W^{(e)}_{k+1/2}$$

Selectable $\alpha_{\min}$ and $\alpha_{\max}$ based on consideration of accuracy and numerical stability of the explicit part.

In the actual code all the above – computing $\alpha = \alpha_{i,j,k}$, then $f(\alpha)$ then splitting W is implanted into the computation of W itself, so none of the intermediates is stored as a 3D array.

Prime in rhs'_k means that the usual r.h.s. computed by ROMS code for the corresponding equations, except the replacement $W_{k+1/2} \to W^{(e)}_{k+1/2}$

$A_{k+1/2}$ is vertical viscosity/diffusion coefficient [including the stabilization terms (Lemarié et. al., 2012) in the case when isoneutral lateral diffusion is used]

The above takes into account kinematic b.c. at surface and bottom, $W_{N+1/2} = W_{1/2} = 0$, bottom no-flux b.c. for tracers. There is an extra term for momentum equation associated with bottom drag which also treated implicitly.

The modified algorithm **retains simultaneous conservation and constancy preservation properties for tracers**, despite the fact that grid box heights change due to changing free surface, $H_k^{n+1} \neq H_k^n$.

The motivation for using upstream discretization for the implicit part comes from the fact that it is monotonic, hence will not cause oscillation. Unavoidably it is diffusive, however this choice is justified by the observation that in practical model solutions large vertical velocities occur only in places with vanishing (or even unstable) stratification and, consequently, already large mixing set by the vertical parameterization scheme.

Well posed, diagonally dominant discrete system.

Fourier analysis

Modified LF-AM3 stepping: predictor

$$q_j^{n+1/2} = \left(\frac{1}{2} - 2\gamma\right) q_j^{n-1} + \left(\frac{1}{2} + 2\gamma\right) q_j^n - i\alpha' (1-2\gamma) \left[\tilde{q}^n_{j+1/2} - \tilde{q}^n_{j-1/2}\right] - i\alpha'' (1-2\gamma) \left[q_j^{n+1/2} - q_{j-1}^{n+1/2}\right]$$

followed by

$$q_j^{n+1} = q_j^n - i\alpha' \left[\tilde{q}^{n+1/2}_{j+1/2} - \tilde{q}^{n+1/2}_{j-1/2}\right] - i\alpha'' \left[q_j^{n+1} - q_{j-1}^{n+1}\right]$$

where

$$\alpha = \frac{c\Delta t}{\Delta x} \qquad \alpha' = \frac{\alpha}{f(\alpha)} \qquad \text{and} \qquad \alpha'' = \alpha - \alpha'$$

$\gamma = 1/12$ for 3rd-order temporal accuracy as usual

Inserting Fourier component $q_j^n = \lambda^n \cdot \widehat{q}_k \cdot e^{ik\Delta x j}$

replacing spatial differencing with $\begin{cases} \tilde{q}_{j+1/2} - \tilde{q}_{j-1/2} = i\mathscr{K}\Delta x \cdot \widehat{q}_k \cdot e^{ik\Delta x j} \\ q_j - q_{j-1} = \left(1 - e^{-ik\Delta x}\right) \cdot \widehat{q}_k \cdot e^{ik\Delta x j} \end{cases}$

yields characteristic equation

$$\left[1 + \alpha''\left(1 - e^{-ik\Delta x}\right)\right]\lambda = 1 - i\alpha'\mathscr{K}\Delta x \cdot \frac{\left(\frac{1}{2} + 2\gamma\right) - i\alpha'\mathscr{K}\Delta x\,(1 - 2\gamma)}{1 + \alpha''\,(1 - e^{-ik\Delta x})\,(1 - 2\gamma)}$$
$$-i\alpha'\mathscr{K}\Delta x \cdot \frac{\left(\frac{1}{2} - 2\gamma\right)}{1 + \alpha''\,(1 - e^{-ik\Delta x})\,(1 - 2\gamma)} \cdot \lambda^{-1}$$

which **can be made unconditionally stable** by parameter choice in limiter function $f(\alpha)$. Note that if $[1 + \alpha''...] \to 1$ the above reverts back to the original LF-AM3 characteristic equation.

LF-AM3-Adaptive, $|\lambda|^{(1/\alpha)}$ $c^*/c^{(\text{exact})}$

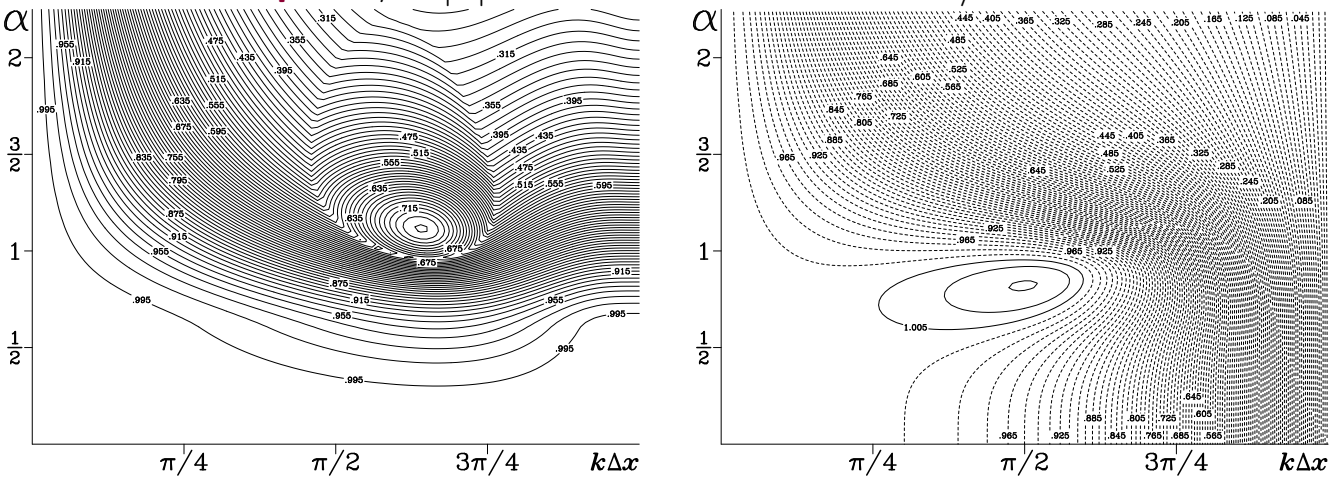

$\alpha_{\min} = 0.6,\ \alpha_{\max} = 1.0$

cf., Fully-Implicit, $|\lambda|^{(1/\alpha)}$ $c^*/c^{(\text{exact})}$

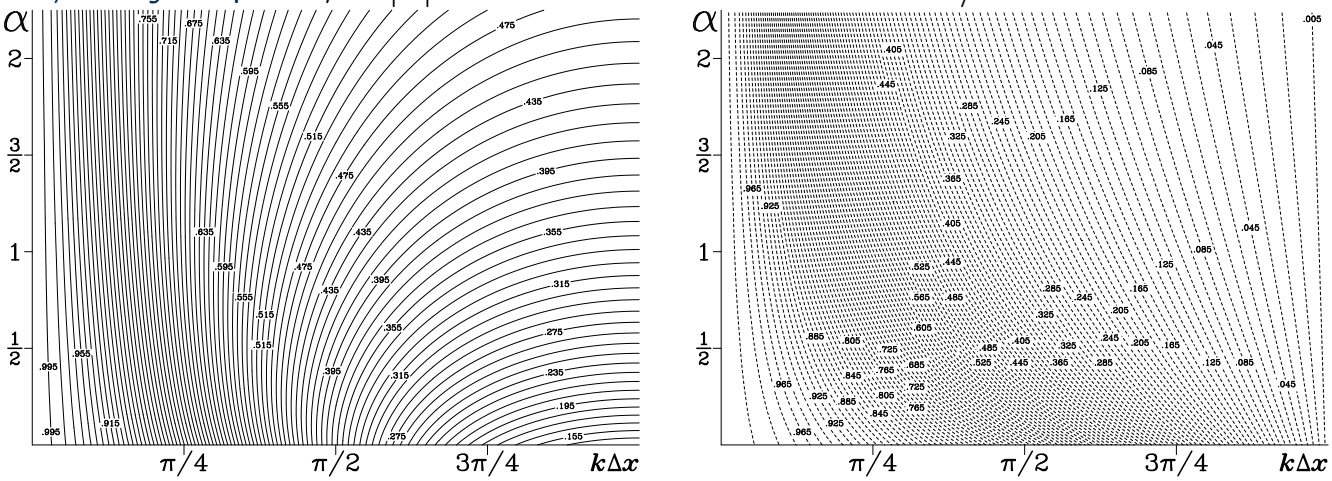

$\alpha_{\min}, \alpha_{\max} \to 0 \quad \Rightarrow$ backward-Euler, upstream in space

For $0 < \alpha \leq \alpha_{\min}$ the algorithm is identical to the original LF-AM3. For $\alpha \to \infty$ it asymptotes to fully implicit. Smooth transition over a wide zone; LF-AM3 phase acceleration toward its stability limit helps.

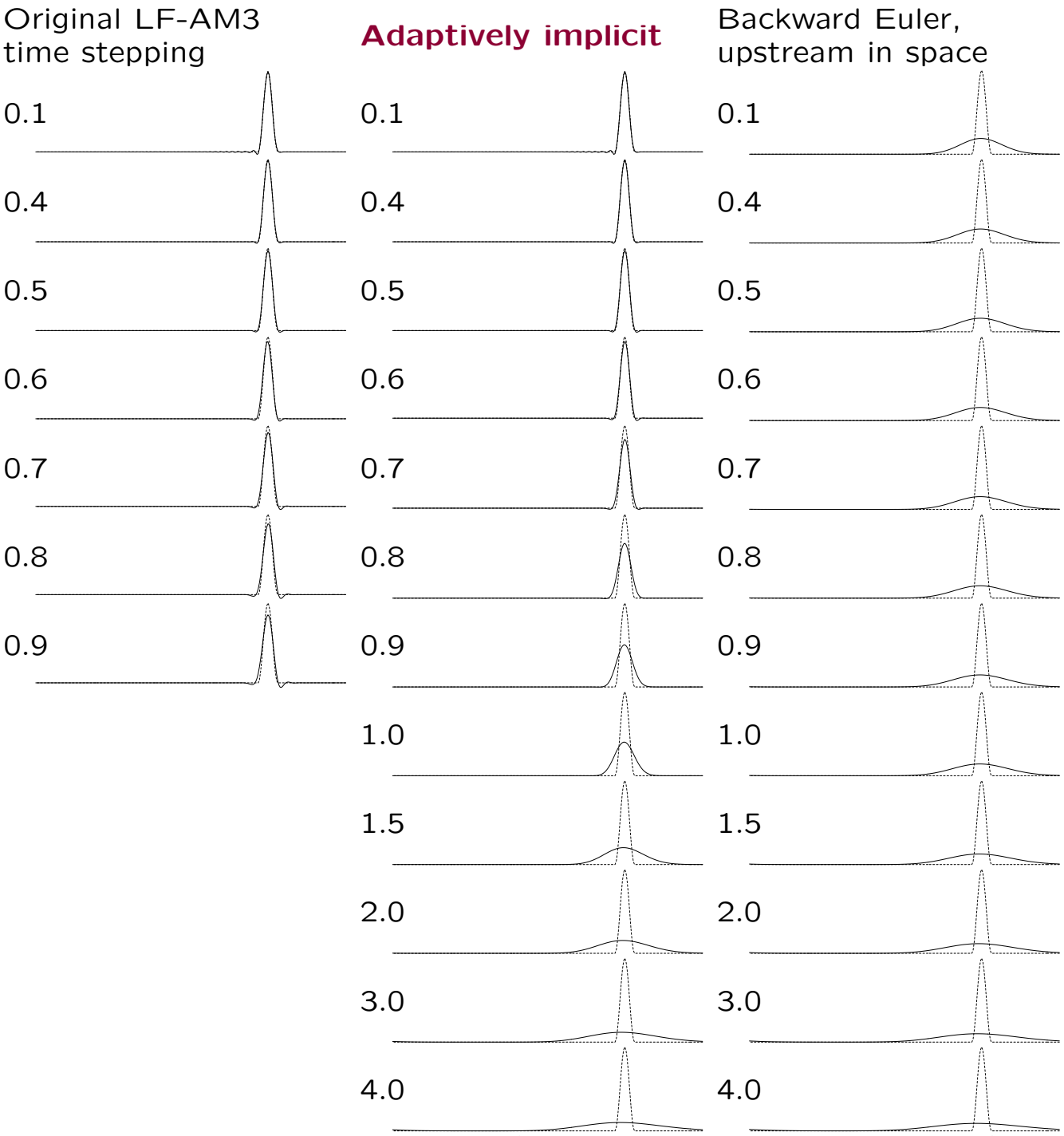

Comparison of LF-AM3 algorithm (*left column*, adaptively implicit (*middle column*, threshold Courant numbers settings $\alpha_{\min} = 0.6$, $\alpha_{\max} = 1.0$), and fully-implicit backward Euler upstream in space advection (*right column*). Number on the left of each panel indicates Courant number.

Test problem: Gravitational adjustment a.k.a. "lock-exchange". Same setup as in Ilıcak et. al. (2012). Also a standard ROMS test problem, Haidvogel & Beckmann (1990). Inspired by Benjamin (1968) classical work. Known for generating sharp fronts with the resulting vertical velocities playing the dominant factor in CFL limitation.

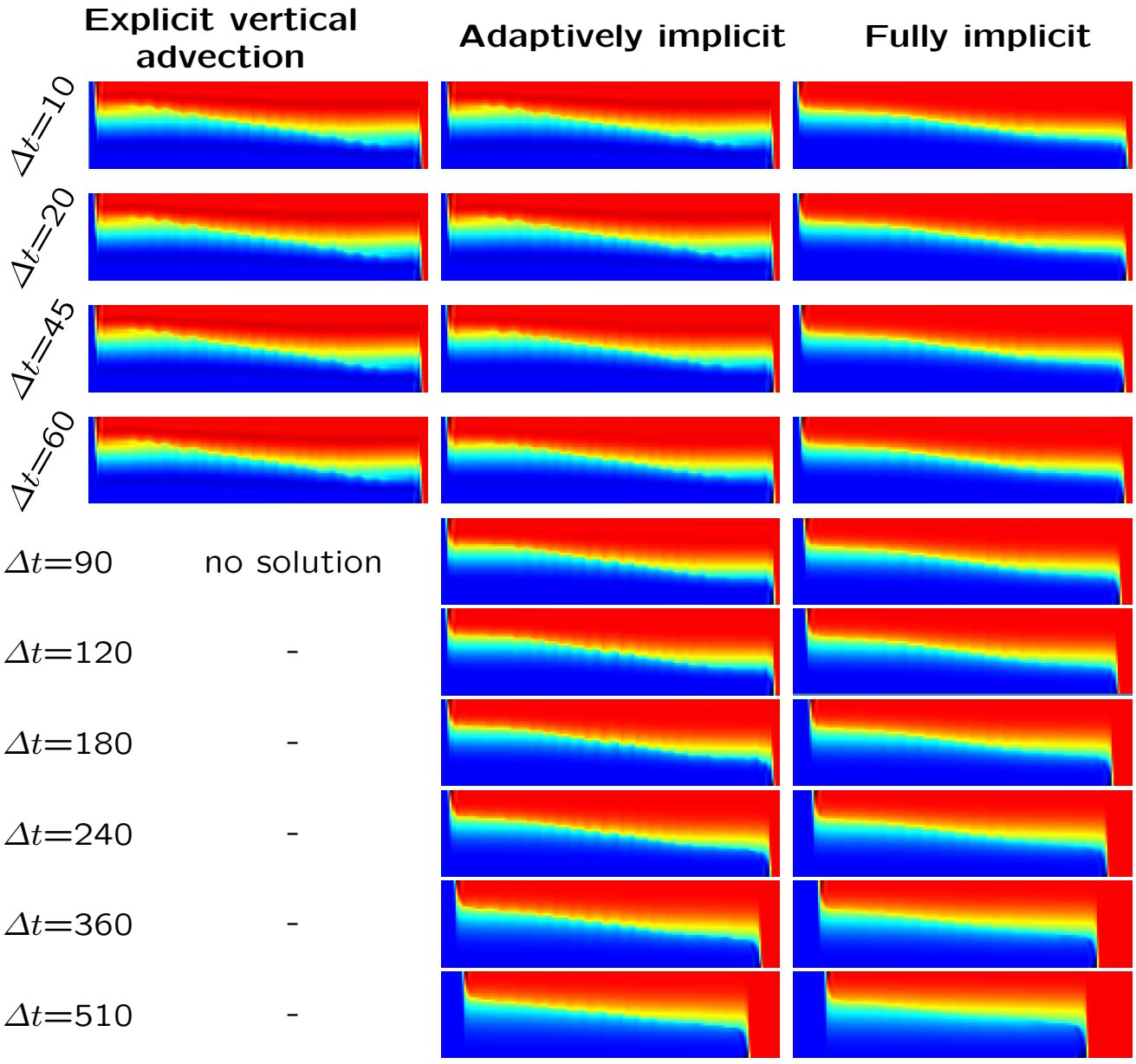

The solution (vertical along-channel xz cross-section of temperature field) is shown at 17 hours since initialization (matches Fig. 2 and Fig. 5 from Ilıcak et. al., 2012). The length of the domain is $64km$, depth is $20m$, grid resolution $\Delta x = 400m$, $\Delta z = 0.5m$. Aspect ratios $\Delta z/\Delta x = 1/800 \ll 1$ and $h/\Delta x = 1/20 \ll 1$ so this grid does admit nonhydrostatic effects. Unlike Ilıcak who selected Smolarkiewicz scheme (the best fit for this particular problem, but is too diffusive for realistic long-term

simulations), we use a third-order upstream scheme in the horizontal, and parabolic splines in vertical (for the explicit part). They also their tests with $\Delta t = 1s$ resulting in vanishingly small CFL, while our goal here is to push it to the limit. Note the progressive delay in the front propagation for the largest Δt – neither adaptive, nor fully implicit scheme is expected to be accurate at this regime ($\Delta t = 240...510s$), but still adaptive shows slightly less delay and less mixing.

Conclusion

- Accurate representation of physical processes **require resolving them in time**: there is no way around it, no miracles.
- Explicit advection algorithm can be designed in such a way that using it close to the largest possible time step allowed by their numerical stability does not compromise the accuracy of the solution.
- Implicit can not. ...at least not the classical θ-method at $\alpha \approx 1/2$.
- ROMS has actually a lot to loose...
- **Adaptive implicit advection is designed as extension to the explicit.**
- Accuracy of the explicit part of algorithm within the useful portion of its stability range is fully retained – **there is no compromise whatsoever**.
- Implicitness activates itself only where and when it is **absolutely necessarily**.
- Seamless transition from fully explicit to partially implicit to more implicit.
- Deliberately **designed to dissipate** what is not resolved by time step.
- **No more blow ups because of vertical over-speeding.**
- **Use wisely:** Courant number is 3D Courant number for the purpose of adaptive control, as is dictated by the overall budget of numerical stability. This means that the explicitness available for vertical direction is what left after been "taxed" by horizontal advection.
- Fits into existing code infrastructure: Modifies computation of W, implicit vertical solvers, and adds implicit solver into ROMS predictor sub-step. very mild increase in overall computational cost.